AIAA JOURNAL
Vol. 32, No. 2, February 1994

Parametric Quadratic Programming Method for Dynamic Contact Problems with Friction

S. M. Sun*
Institute of Space and Astronautical Science, Yoshinodai, Sagamihara 229, Japan
H. S. Tzou†
University of Kentucky, Lexington, Kentucky 40506
and
M. C. Natori‡
Institute of Space and Astronautical Science, Yoshinodai, Sagamihara 229, Japan

Based on the parametric variational principle, a general but effective parametric quadratic programming technique satisfying various contact conditions is established for dynamic analysis of contact problems with friction and damping. The discretization with respect to time and space leads to a static linear complementary problem (LCP) for each time step which is solved by a quadratic optimization algorithm such as the Lemke algorithm, etc. Thus, the convergence and numerical stability of the solution can be guaranteed. The substructure condensation technique is implemented to handle the unknown contact boundary condition so that the computation effect is considerably reduced. As an application of the method presented, three dynamic contact examples and numerical results are given.

I. Introduction

CONTACT problems are of great importance in engineering applications. Because of the inherent nonlinearity of contact problems, they are generally difficult to solve analytically. Numerical solutions using the finite element method seem to be an attractive alternative. Significant efforts are devoted to the development of efficient algorithms.

This study is concerned with the numerical analysis of a class of problems in contact dynamics in which friction and damping effects are taken into account. The finite element method is used herein to analyze the dynamic behavior of elastic contact bodies. Time-dependent contact regions exist for the dynamic contact process. Numerical algorithms are necessary to calculate all time-dependent quantities during this process. This leads to an iterative algorithm for the determination of contact regions and stresses in each time step. Previously published algorithms dealing with dynamic contact problems can be broadly categorized into two types: the incremental iterative method[1-7] and the mathematical programming method.[8-10] The present paper belongs to the second type.

In the static contact analysis, it has been noted that the algorithms, based upon the parametric quadratic programming technique, can guarantee not only the convergence of the solution but also the numerical stability.[11-14] Therefore, the purpose of this paper is to extend the parametric quadratic programming method to accommodate the dynamic contact problem. According to the parametric variational principle, the incremental functional with the parametric vector can be expressed as a dynamic variational functional. In addition, the relation between the forces and displacements of the contact interfaces is discussed, and contact element and contact constitutive model are introduced. By discretizing the variational functional with respect to time and using the finite element method, the linear complementary problem at each time step solving the dynamic contact problem is obtained. In order to reduce the computer cost, the substructure condensation technique for determining the unknown contact region is used.

Finally, three numerical examples are carried out to demonstrate the validity and applicability of the method developed. These include the contact-impact problem of bars, the beam-mass-beam system with the initial gap and damping, and the triangular rigid-punch problem. Favorable agreement between the present results and referenced solutions is noted.

II. Theoretical Model

Figure 1 shows the contact problem considered with two contact bodies Ω_1 and Ω_2 ($\Omega = \Omega_1 + \Omega_2$). Their boundaries can be decomposed into

$$\Gamma^{(\alpha)} = \Gamma_p^{(\alpha)} \cup \Gamma_u^{(\alpha)} \cup \Gamma_c^{(\alpha)} \qquad \alpha = 1,2 \tag{1}$$

where $\Gamma_c^{(\alpha)}$ are the parts of the boundaries where displacements are prescribed. External loads are dynamically applied at $\Gamma_p^{(1)}$ and $\Gamma_p^{(2)}$ at each time step. In addition to the already-mentioned boundary parts, boundaries $\Gamma_c^{(\alpha)}$ ($\alpha = 1,2$) are set on which the unilateral boundary conditions and Coulomb's friction conditions are prescribed. For two-dimensional dynamical contact problems, the contact states in $\Gamma_c^{(\alpha)}$ at each time step k are classified according to three categories, which are

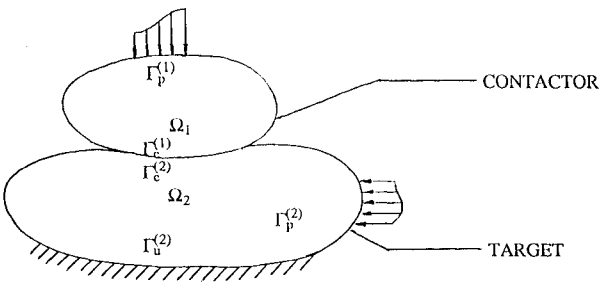

Fig. 1 Contact of two elastic bodies.

Received Feb. 10, 1993; presented as Paper 93-1388 at the AIAA/ASME/ASCE/AHS/ASC 34th Structures, Structural Dynamics, and Materials Conference, La Jolla, CA, April 19-21, 1993; revision received June 7, 1993; accepted for publication June 9, 1993.

*Visiting Research Fellow on leave from Dalian University of Technology, Dalian, 116023, People's Republic of China.
†Associate Professor of Mechanical Engineering. Member AIAA.
‡Professor of Spacecraft Engineering. Member AIAA.

defined by inequalities in the contact local coordinate system O-$n\tau$ as follows:

1) Free state when the two bodies are separated

$$\Delta u_n^{(2)} - \Delta u_n^{(1)} + \delta^*(t_{k-1}) > 0 \tag{2}$$

2) Sticking state when the two bodies are in contact and no sliding occurs

$$\begin{aligned} &\Delta u_n^{(2)} - \Delta u_n^{(1)} + \delta^*(t_{k-1}) = 0, \qquad p_n(t_{k-1}) + \Delta p_n < 0 \\ &|\Delta u_\tau^{(2)} - \Delta u_\tau^{(1)}| = 0, \qquad |p_\tau(t_{k-1}) + \Delta p_\tau| < -\mu \cdot [p_n(t_{k-1}) + \Delta p_n] \end{aligned} \tag{3}$$

3) Sliding state when the two bodies are in contact and sliding occurs

$$\begin{aligned} &\Delta u_n^{(2)} - \Delta u_n^{(1)} + \delta^*(t_{k-1}) = 0, \qquad p_n(t_{k-1}) + \Delta p_n < 0 \\ &|\Delta u_\tau^{(2)} - \Delta u_\tau^{(1)}| > 0, \qquad |p_\tau(t_{k-1}) + \Delta p_\tau| = -\mu \cdot [p_n(t_{k-1}) + \Delta p_n] \end{aligned} \tag{4}$$

In the preceding expressions, $u_\tau^{(\alpha)}$, $u_n^{(\alpha)}$, and p_τ, p_n are the tangent and normal displacements and the tangent and normal forces with respect to the contact local coordinates, respectively. Terms μ and δ^* denote the dynamical friction coefficient and contact gap, respectively. For symbol convenience, $\Delta(\cdot)$ indicates the incremental values, and $(\cdot)(t_{k-1})$ and $(\cdot)(t_k)$ represent those values at time steps $k-1$ and k, respectively. Thus the following operator relation is valid:

$$(\cdot)(t_k) = (\cdot)(t_{k-1}) + \Delta(\cdot) \tag{5}$$

By choosing the penalty method[11-14] the constraint conditions (2-4) are relaxed, so that we have the approximate expressions for the tangent and normal parts of the interface force

$$p_n(t_{k-1}) + \Delta p_n = \begin{cases} -E \bullet [\Delta u_n^{(1)} - \Delta u_n^{(2)} - \delta^*(t_{k-1})], & \text{for both sticking and sliding states} \\ 0, & \text{for free state} \end{cases} \tag{6}$$

$$p_\tau(t_{k-1}) + \Delta p_\tau = \begin{cases} -E \bullet (\Delta u_\tau^{(2)} - \Delta u_\tau^{(1)}), & \text{for sticking state} \\ -\mu \bullet (p_n(t_{k-1}) + \Delta p_n] \bullet \operatorname{sign}(\Delta u_\tau^{(2)} - \Delta u_\tau^{(1)}), & \text{for sliding state} \end{cases} \tag{7}$$

Obviously, the interface force depends on a real parameter E, the so-called penalty factor. To this end, the contact element can be introduced into the regular, nonlinear finite elements and has the stiffness matrix $\boldsymbol{K}_c^e$ for incremental contact displacement vector $\Delta \boldsymbol{u}_c^e$. In this paper, we employ the superscript e to denote the quantity in the elemental level

$$\boldsymbol{K}_c^e = \begin{bmatrix} E & 0 \\ 0 & E \end{bmatrix} \tag{8}$$

$$\Delta \boldsymbol{u}_c^e = \{\Delta u_\tau^{(2)} - \Delta u_\tau^{(1)} \; \Delta u_n^{(2)} - \Delta u_n^{(1)} + \delta^*(t_{k-1})\}^T \tag{9}$$

On the other hand, we apply a plasticity-like dissipative functional approach to model friction and normal contact phenomenon. Hence, the approach consists of assuming that three slip (or yielding) functions exist for each contact pair.

$$\begin{aligned} f_1 &= p_\tau + \mu p_n \le 0 \\ f_2 &= -p_\tau + \mu p_n \le 0 \\ f_3 &= p_n \le 0 \end{aligned} \tag{10}$$

Based on a framework for the plasticity theory of friction, the split of the incremental displacement $\Delta \boldsymbol{u}_c^e$ on the contact surface is adopted, that is,

$$\Delta \boldsymbol{u}_c^e = \Delta \boldsymbol{u}_c^r + \Delta \boldsymbol{u}_c^p \tag{11}$$

where $\Delta \boldsymbol{u}_c^r$ and $\Delta \boldsymbol{u}_c^p$ are the elastic and sliding parts of $\Delta \boldsymbol{u}_c^e$, respectively. In fact, the elastic incremental contact displacement $\Delta \boldsymbol{u}_c^r$ is defined as that part where the sliding does not occur. With these assumptions at hand, the sliding contact displacement $\Delta \boldsymbol{u}_c^p$ can be determined as follows:

$$\Delta u_{ci}^p = (\lambda^e)^T \frac{\partial (\boldsymbol{g}^e)^T}{\partial p_i} \qquad i = n, \tau \tag{12}$$

Here, $\lambda^e = \{\lambda_1 \; \lambda_2 \; \lambda_3\}^T$ is the flow parameter vector, and $\boldsymbol{g}^e = \{g_1 \; g_2 \; g_3\}$ is the slip potential function vector. Since the component g_i ($i = 1,2,3$) is defined in Eq. (13), it implies that g_i corresponds to the yielding function f_i.

$$\begin{aligned} g_1 &= p_\tau \\ g_2 &= -p_\tau \\ g_3 &= p_n \end{aligned} \tag{13}$$

In addition, the contact force $\boldsymbol{p}_c^e = \{p_\tau \; p_n\}^T$ for each contact element satisfies the following force-displacement relation:

$$\boldsymbol{p}_c^e = \boldsymbol{K}_c^e \Delta \boldsymbol{u}_c^r = \boldsymbol{K}_c^e (\Delta \boldsymbol{u}_c^e - \Delta \boldsymbol{u}_c^p) \tag{14}$$

Thus, the contact force $\boldsymbol{p}_c^e$ follows from Eqs. (11), (12), and (14)

$$\boldsymbol{p}_c^e = \boldsymbol{K}_c^e \Delta \boldsymbol{u}_c^e - \lambda^e \Phi^e \tag{15a}$$

where Φ^e is known as the gradient matrix, which can be given by

$$\Phi^e = \boldsymbol{K}_c^e \frac{\partial (\boldsymbol{g}^e)^T}{\partial \boldsymbol{p}_c^e} \tag{15b}$$

For computer implementation purposes, the yielding function vector $\boldsymbol{f}^e = \{f_1 f_2 f_3\}^T$, which is given by Eq. (10), requires linearization via

$$\boldsymbol{f}^e = \boldsymbol{f}^e(t_k) \approx \boldsymbol{f}^e(t_{k-1}) + \frac{\partial \boldsymbol{f}^e}{\partial \boldsymbol{p}_c^e} \Delta \boldsymbol{p}_c^e \le 0 \tag{16}$$

By recalling the contact force relation (15), the inequality (16) can be expressed in the following form:

$$\boldsymbol{f}^e(t_{k-1}) - \frac{\partial \boldsymbol{f}^e}{\partial \boldsymbol{p}_c^e} \boldsymbol{p}_c^e(t_{k-1}) + \boldsymbol{S}^e \Delta \boldsymbol{u}_c^e - \boldsymbol{H}^e \lambda^e \le 0 \tag{17}$$

where

$$\boldsymbol{S}^e = \frac{\partial \boldsymbol{f}^e}{\partial \boldsymbol{p}_c^e} \boldsymbol{K}_c^e, \qquad \boldsymbol{H}^e = \frac{\partial \boldsymbol{f}^e}{\partial \boldsymbol{p}_c^e} \boldsymbol{K}_c^e \frac{\partial (\boldsymbol{g}^e)^T}{\partial \boldsymbol{p}_c^e} \tag{18}$$

It should be noted that the parameter λ_i ($i = 1,2,3$) must satisfy the following conditions:

$$\lambda_i = \begin{cases} 0, & \text{if } f_i \le 0 \\ \ge 0, & \text{if } f_i = 0 \end{cases} \tag{19}$$

A complementary problem (20) can be obtained by introducing the so-called slack variable ν_i ($i = 1,2,3$) into Eqs. (17-19)

$$\begin{aligned} &\nu^e + \boldsymbol{S}^e \Delta \boldsymbol{u}_c^e = \boldsymbol{H}^e \lambda^e + \boldsymbol{d}^e \\ &\lambda^e \cdot (\nu^e)^T = 0, \qquad \lambda^e, \nu^e \ge 0 \end{aligned} \tag{20}$$

in which the tolerance vector of the contact element is calculated by

$$d^e = f^e(t_{k-1}) - \frac{\partial f^e}{\partial p_c^e} p_c^e(t_{k-1}) \tag{21}$$

The complementary condition (20) represents the following behaviors at every time step k: 1) the contactor cannot penetrate the target body; 2) the contact pressure is negative and different from zero only if the two bodies are in contact; and 3) the contact pressure and tangential force satisfy Coulomb's friction law.

III. Finite Element Formulation

Since the sliding contact with friction is a nonconservative process, an incremental parametric variational principle is derived in this paper. For both contactor Ω_1 and target body Ω_2 as shown in Fig. 1, it is assumed that the variables of the system are known from the instant t_0 up to the instant t_{k-1}. Further, the variables of the system are separated into two groups: the state variables such as stresses, displacements, velocities, accelerations, etc. and the control variables, i.e., parametric variables λ_i in the complementary problem (19). Because the instant t_{k-1} is infinitesimally close to the instant t_k, all governing equations may be linearized with respect to the increments. Hence, the equilibrium configuration at the time step k is achieved when the incremental displacement field minimizes the incremental functional $\Delta\pi$. According to the parametric variational principle,[8,11-15] the parametric variable λ_i is treated as a parameter not subject to variation. By taking the variation with respect to the admissible incremental displacement field between t_{k-1} and t_k, we have

$$\begin{aligned}\delta\Delta\pi = \int_{t_{k-1}}^{t_k} \Bigg\{ \int_\Omega \rho[\ddot{u}_i(t_{k-1}) + \Delta\ddot{u}_i]\delta\Delta u_i \, d\Omega + \int_\Omega [\sigma_{ij}(t_{k-1}) \\ + \Delta\sigma_{ij}]\delta\Delta\epsilon_{ij} \, d\Omega - \int_\Omega [\bar{b}_i(t_{k-1}) + \Delta\bar{b}_i]\delta\Delta u_i \, d\Omega - \int_{\Gamma_p} [\bar{p}_i(t_{k-1}) \\ + \Delta\bar{p}_i]\delta\Delta u_i \, dS + \int_\Omega [\bar{c}_i(t_{k-1}) + \Delta\bar{c}_i]\delta\Delta u_i \, d\Omega + \int_{\Gamma_c} [p_{ci}(t_{k-1}) \\ + \Delta p_{ci}]\delta\Delta u_i \, dS \Bigg\} dt = 0\end{aligned} \tag{22}$$

where ρ, $\ddot{u}_i$, σ_{ij}, ϵ_{ij}, $\bar{b}_i$, $\bar{p}_i$, and $\bar{c}_i$ denote material density, acceleration, stress tensor, strain tensor, body force, traction, and damping force, respectively. In addition, it should be pointed out that the variational form of Eq. (22) is subject to the normal and tangential frictional constraints given by Eqs. (10) or (17).

In the usual manner for finite element discretizations, the incremental displacement field is approximated by using an elementwise separation of variables, so that

$$\Delta u_i = \sum_I N_I^e \Delta u_{iI}^e = N^e \Delta u^e \tag{23}$$

where Δu^e is related to the global matrix of nodal incremental displcements by the Boolean connectivity matrix L^e

$$\Delta u^e = L^e \Delta u \tag{24}$$

It is also convenient to use the assembled shape function N, say,

$$N = \bigcup_{e=1}^{ne} N^e L^e \tag{25}$$

Here the structure Ω is discretized by ne finite elements and nc contact elements; therefore, we can write

$$\Delta u_i = N \Delta u \tag{26}$$

If we introduce the approximation (26) in variational equality (22), the problem (22) can be rearranged as the matrix form

$$\begin{aligned}\delta\Delta\pi = \int_{t_{k-1}}^{t_k} \{ M[\ddot{u}(t_{k-1}) + \Delta\ddot{u}] + F(t_{k-1}) + \Delta F - P(t_{k-1}) \\ - \Delta P + C[\dot{u}(t_{k-1}) + \Delta\dot{u}] + K_c \Delta u - \Phi\lambda \}\delta\Delta u \, dt = 0\end{aligned} \tag{27}$$

To this end, we have introduced the following matrix notations: u, $\dot{u}$, $\ddot{u}$ are the column vectors of nodal displacements, velocities, and accelerations, respectively; and M is the lumped mass matrix, F the internal force vector, P the external force vector (body forces and prescribed tractions), and C the damping matrix. Thus, we satisfy

$$C[\dot{u}(t_{k-1}) + \Delta\dot{u}] = \bigcup_{e=1}^{ne} \int_{\Omega^e} N^T[\bar{c}_i(t_{k-1}) + \Delta\bar{c}_i] \, d\Omega \tag{28}$$

when K_c is the global contact stiffness matrix and Φ the global potential matrix, which can be expressed as

$$\Phi = \bigcup_{e=1}^{nc} \int_{\Gamma_c^e} N^T \Phi^e \, dS \tag{29}$$

Clearly, the virtual incremental $\delta\Delta u$ is arbitrary, which implies that it can be assigned values at will. Because the integral must vanish for all values of $\delta\Delta u$, Eq. (27) can be satisfied if and only if the coefficient of $\delta\Delta u$ is equal to zero, or

$$\begin{aligned}M\Delta\ddot{u} + C\Delta\dot{u} + \Delta F + K_c\Delta u = [P(t_{k-1}) - M\ddot{u}(t_{k-1}) \\ - C\dot{u}(t_{k-1}) - F(t_{k-1}) + \Delta P] + \Phi\lambda\end{aligned} \tag{30}$$

The internal force ΔF generated from the incremental displacement Δu can be approximated by the multiplication of the stiffness matrix K_n and Δu, say,

$$\Delta F = K_n \Delta u \tag{31}$$

From Eq. (31), the equation of motion (30) takes the form

$$M\Delta\ddot{u} + C\Delta\dot{u} + K\Delta u = R + \Phi\lambda \tag{32a}$$

with

$$K = K_n + K_c \tag{32b}$$

$$R = P(t_{k-1}) - M\ddot{u}(t_{k-1}) - C\dot{u}(t_{k-1}) - F(t_{k-1}) + \Delta P \tag{32c}$$

IV. Dynamic Contact Analysis

The numerical solution of the dynamic contact problems with friction is obtained by discretizing the incremental functional $\Delta\pi$ with the parametric vector λ with respect to time and space, and by taking into account the initial conditions $u(t_0) = u_0$, $\dot{u}(t_0) = \dot{u}_0$, $\ddot{u}(t_0) = \ddot{u}_0$. In the following paragraphs we discuss some aspects concerning the time integration and show that the solution of Eq. (32) is obtained by solving a static complementary problem at each time step k.

At first, it should be pointed out that of the existing time integration schemes only the direct integration method can be used. In this paper, the Newmark time integration scheme is adopted with some modifications to accommodate the dynamic contact problems. Because the variables of the system are known from the instant t_0 up to the instant t_{k-1}, we can compute the displacement and kinematic field at the instant t_k as

$$\begin{aligned}\ddot{u}(t_k) &= \frac{u(t_{k+1}) - u(t_{k-1})}{\beta\Delta t^2} + \left(1 - \frac{1}{2\beta}\right)\ddot{u}(t_{k-1}) - \frac{\dot{u}(t_{k-1})}{\beta\Delta t} \\ \dot{u}(t_k) &= \frac{u(t_k) - u(t_{k-1})}{2\beta\Delta t} + \left(1 - \frac{1}{4\beta}\right)\ddot{u}(t_{k-1})\Delta t + \left(1 - \frac{1}{2\beta}\right)\dot{u}(t_{k-1}) \\ u(t_k) &= u(t_{k-1}) + [u(t_k) - u(t_{k-1})] \\ \Delta t &= t_k - t_{k-1}\end{aligned} \tag{33}$$

where β is Newmark parameter. If we write Eqs. (33) in the incremental form, they lead to

$$\Delta\ddot{u} = \ddot{u}(t_k) - \ddot{u}(t_{k-1}) = \frac{\Delta u}{\beta\Delta t^2} - \frac{\ddot{u}(t_{k-1})}{2\beta} - \frac{\dot{u}(t_{k-1})}{\beta\Delta t}$$

$$\Delta\dot{u} = \dot{u}(t_k) - \dot{u}(t_{k-1}) = \frac{\Delta u}{2\beta\Delta t} + \left(1 - \frac{1}{4\beta}\right)\ddot{u}(t_{k-1})\Delta t - \frac{\dot{u}(t_{k-1})}{2\beta} \quad (34)$$

$$\Delta u = u(t_k) - u(t_{k-1}) = \Delta u$$

Substitution of Eq. (34) into Eq. (32a) yields for t_{k-1}

$$\left(\frac{M}{\beta\Delta t^2} + \frac{C}{2\beta\Delta t} + K\right)\Delta u - \Phi\lambda - \left[R + \frac{M\ddot{u}(t_{k-1})}{2\beta} + \frac{M\dot{u}(t_{k-1})}{\beta\Delta t} - \left(1 - \frac{1}{4\beta}\right)C\ddot{u}(t_{k-1})\Delta t + \frac{C\dot{u}(t_{k-1})}{2\beta}\right] = 0 \quad (35)$$

For the assembled structure, the complementary problem (20) can be rewritten as follows:

$$S\Delta u - H\lambda - d + v = 0$$
$$\lambda \bullet v^T = 0, \qquad \lambda, v \geq 0 \quad (36)$$

where S, H, and d are the global contact constraint matrix, contact resistance matrix, and contact tolerance vector, respectively, and they are evaluated by

$$S = \bigcup_{e=1}^{nc} \int_{\Gamma_c^e} S^e N \, dS, \quad H = \bigcup_{e=1}^{nc} \int_{\Gamma_c^e} H^e \, dS, \quad d = \bigcup_{e=1}^{nc} \int_{\Gamma_c^e} d^e \, dS \quad (37)$$

Substituting Eq. (35) into the problem (36) results in the following linear complementary problem:

$$v - (H - S\bar{K}^{-1}\Phi)\lambda = -S\bar{K}^{-1}\bar{R} + d$$
$$\lambda \bullet v^T = 0, \qquad \lambda, v \geq 0 \quad (38)$$

where

$$\bar{K} = \frac{M}{\beta\Delta t^2} + \frac{C}{2\beta\Delta t} + K \quad (39)$$

$$\bar{R} = R + \frac{M\ddot{u}(t_{k-1})}{2\beta} + \frac{M\dot{u}(t_{k-1})}{\beta\Delta t} - \left(1 - \frac{1}{4\beta}\right)C\ddot{u}(t_{k-1})\Delta t + \frac{C\dot{u}(t_{k-1})}{2\beta} \quad (40)$$

Therefore, the solution of the dynamic contact problem consists of the solution at each time step of the linear complementary problem (38-40).

V. Solution Method

In the penalty function method, the contact displacement is computed by dividing the violations of the constraint conditions with a large number E called the penalty factor. Because we can see from the preceding derivations that the penalty factor E acts like a modulus, and that it exists in the matrices associated with the contact element, e.g., S, Φ, H, and K_c, the main difficulty for this method is to select as good a penalty factor to satisfy the contact constraint as is possible. A poor penalty may lead to ill conditioning of the direct solution for the linear complementary problem (38-40). However, a noteworthy feature is that although the penalty factor E is applied in the previous sections, it can be eliminated algebraically in solving the linear complementary problem. This is due to the use of an asymptotic generalized inverse of the solution matrix $\bar{K}$.

Similarly to the static contact problems, we divide the global incremental nodal displacement Δu into two groups: the Δu_n of the noncontact nodes (including those in the contactor body) and the incremental contact displacement Δu_c, i.e.,

$$\Delta u = \{\Delta u_n \; \Delta u_c\}^T \quad (41)$$

Hence the matrices $\bar{K}$, S, and Φ and the vector $\bar{R}$ corresponding to the incremental displacement Δu become

$$\bar{K} = \begin{bmatrix} \bar{K}_{11} & \bar{K}_{12} \\ \bar{K}_{21} & \bar{K}_{22} + E \cdot I \end{bmatrix}, \qquad \bar{R} = \{\bar{R}_1, \bar{R}_2\}^T$$
$$S = [0 \; E\bar{S}], \qquad \Phi = \begin{bmatrix} 0 \\ E\bar{\Phi} \end{bmatrix} \quad (42)$$

Applying some special technique,[11-14] an asymptotic generalized inverse of $\bar{K}$ such as $E \to \infty$ can be obtained

$$\bar{K}^{-1} = \begin{bmatrix} \bar{K}_{11}^{-1} & -\frac{1}{E}\bar{K}_{11}^{-1}\bar{K}_{12} \\ -\frac{1}{E}\bar{K}_{21}\bar{K}_{11}^{-1} & \frac{1}{E}I - \frac{1}{E^2}\bar{K}_{22} + \frac{1}{E^2}\bar{K}_{21}\bar{K}_{11}^{-1}\bar{K}_{12} \end{bmatrix} \quad (43)$$

With the preceeding generalized inverse and condition $H = \bar{S} \cdot \bar{\Phi}$ (Refs. 11 and 12), we can establish the following linear complementary problem without the penalty factor E, that is,

$$v - \bar{S}\bar{K}_c\Phi\lambda = \bar{S}\bar{R}_c + d$$
$$v \bullet \lambda^T = 0, \qquad v, \lambda \geq 0 \quad (44)$$

where

$$\bar{K}_c = \bar{K}_{22} - \bar{K}_{21}\bar{K}_{11}^{-1}\bar{K}_{12} \quad (45)$$

$$\bar{R}_c = \bar{R}_2 - \bar{K}_{21}\bar{K}_{11}^{-1}\bar{R}_1 \quad (46)$$

It is obvious that the system is condensed to the potential contact region in Eqs. (45) and (46). In most applications the contact region is small compared to the domain of the structure; therefore, it is a fact that the computational efforts for the dynamic contact analysis can be considerably reduced because the scale of the problem (44-46) is related only to the dimension of the incremental contact displacement Δu_c of the contact pairs.

Suppose that at time t_0 no nodes are in contact. Then the algorithm of the dynamic contact analysis is implemented in the following way:

1) Set $k = 0$, $u(t_0) = u_0$, $\dot{u}(t_0) = \dot{u}_0$, $\ddot{u}(t_0) = \ddot{u}_0$.

2) Compute the matrices without the penalty factor $\bar{S}$, $\bar{\Phi}$, $\bar{K}_{21}$, $\bar{K}_{11}^{-1}$, $\bar{K}_{22}$, and $\bar{K}_c$.

3) Evaluate the force $\bar{R}$ and form the condensed load vector $\bar{R}_c$.

4) Establish the linear complementary problem (44).

5) Solve the problem (44) by means of the Lemke method.

6) Perform and solve for Δu using the equivalent static problem

$$\bar{K}\Delta u = \bar{R} \quad (47)$$

7) Compute the nodal velocities and accelerations at the time step k according to Eq. (33).

8) If $k = k + 1$, go to step 2.

If the time interval Δt at each time step k is equal and the deformation in which the stiffness matrix $\bar{K}$ does not change is small, it is not necessary for each time step to make the dynamic condensation. In that case, the computations of $\bar{S}$, $\bar{\Phi}$, $\bar{K}_{21}$, $\bar{K}_{11}^{-1}$, $\bar{K}_{22}$, $\bar{K}_c$ at step 2 can be considered constant matrices. In addition, this algorithm is stable and conservative except for the loss of energy which occurs in the determination of the time t_{k-1}.

VI. Verification Problems

To assess the accuracy of the algorithm, three test problems are analyzed, and results are compared with known analytical solutions.

Contact-Impact of Two Elastic Bars

In this first test problem we consider two bars colliding with each other. As shown in Fig. 2, an elastic bar with the initial velocity 0.1 cm/s collides with another bar rest. Their dimensions and properties are L_1, A_1, E_1, and ρ_1 for the bar 1 and L_2, A_2, E_2, and ρ_2 for the bar 2. Here L_i, A_i, E_i, and ρ_i ($i = 1,2$) are the length, cross-sectional area, modulus of elasticity, and material density, respectively. For verification, the dimensions of both bars as well as the material constants are shown in Table 1. These values are consistent with any system of units. Each bar is discretized into 40 elements, and time increment Δt is taken as 0.005 s.

The analytical solution of the contact time is given by $CT = 2L(\rho/E)^{1/2}$. Therefore, and according to the given data, $CT = 0.2$ s. The contact time obtained with the present algorithm is 0.205 s, and the error with respect to the analytical solution is 2.5%. Figure 3 shows the displacements of the contact points vs time. The results, which were obtained by the direct simulation method[5] and Mahmoud et al.,[9] are also shown for comparison purposes. Excellent agreement can be found.

If we change the modulus of bar 1 to $E_1 = 49$ kgf/cm^2, the displacements of contact points vs time is shown in Fig. 4. The contact times obtained by Ref. 9 and the present paper are 0.2763634 s and 0.275 s, respectively. As is evident, the change of E_1 extends the contact time.

The displacement signatures of the contact interface between the two bars (Figs. 3 and 4) show the importance of the impact and release conditions. The impact condition brings the contact between two bars, and the displacements of the

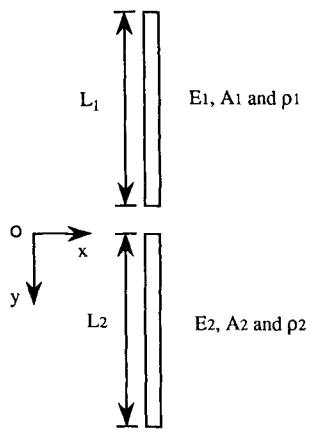

Fig. 2 Normal impact of two bars.

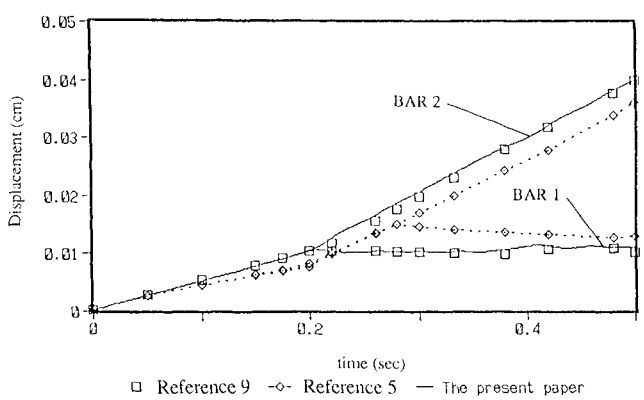

Fig. 3 Transient response of the contact surface for two identified bars.

Table 1 Constants of identical elastic bars

Young's modulus, kg·cm^{-1}·s^{-2}	100
Length, cm	10
Material density, kg·cm^{-3}	0.01
Cross-sectional area, cm^2	1

Table 2 Natural frequencies of H structure, Hz

Method mode	Analytical solution	SAP-IV[1]	NDAFEP[1]	NAS-JIGFEX
1	6.9996	6.8275	6.8289	6.8247
2,3	240.2	233.8	233.9	234.8
4,5	629.7	628.8	629.8	614.7

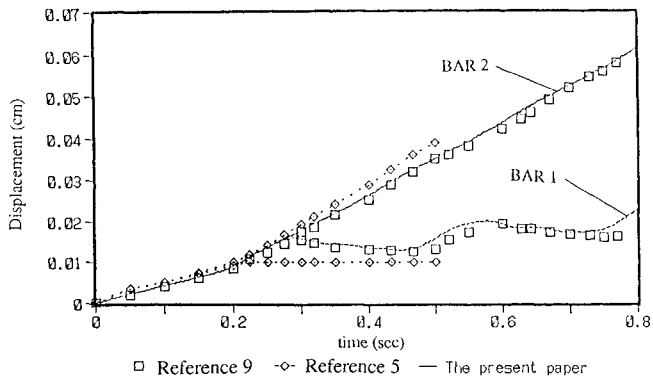

Fig. 4 Transient response of the contact surface for two dissimilar bars.

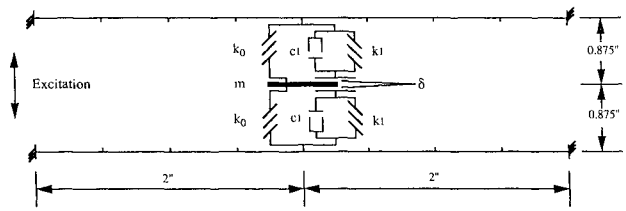

Fig. 5 Finite element model of an H structure.

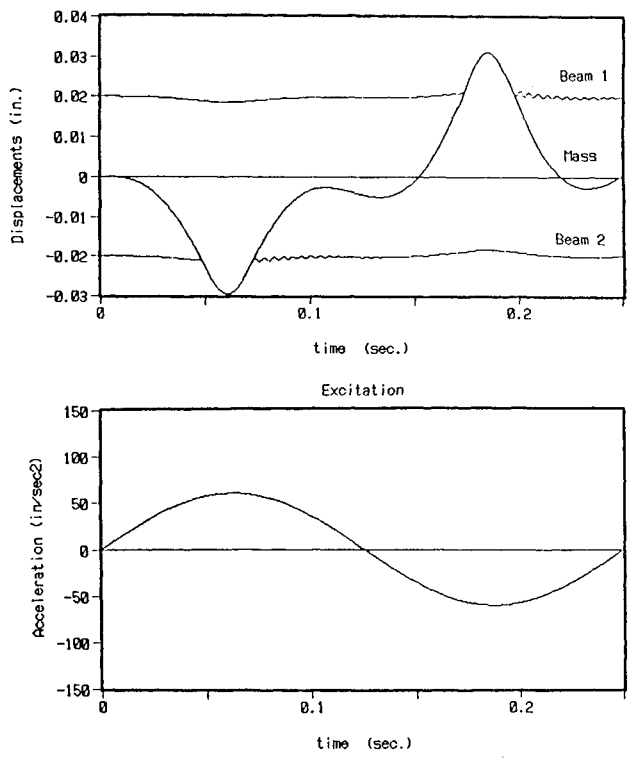

Fig. 6 Dynamic response of an H structure at 4-Hz base excitation.

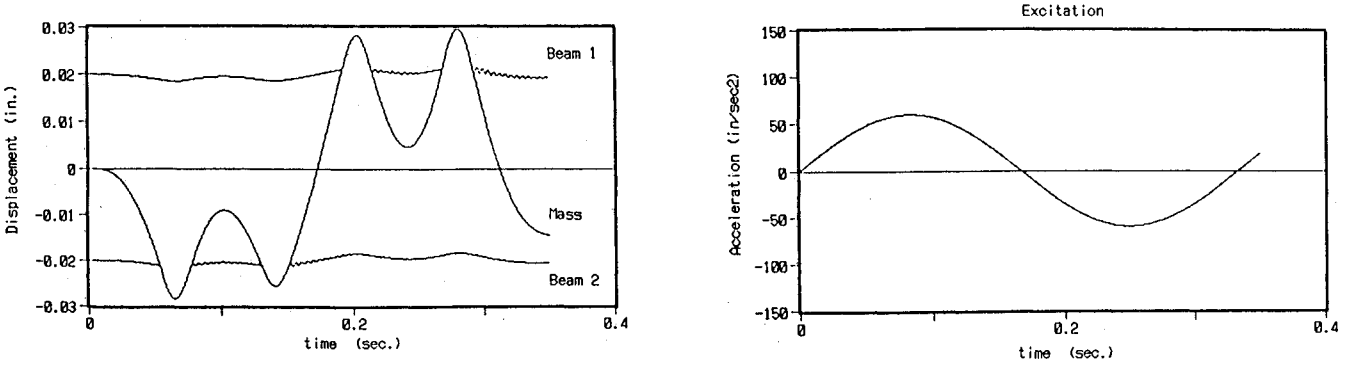

Fig. 7 Dynamic response of an H structure at 3-Hz base excitation.

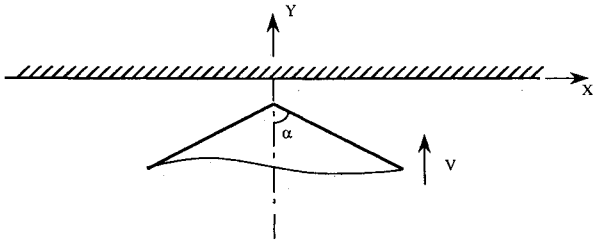

Fig. 8 Rigid triangular punch driven into a half-plane.

Table 3 Computation data for triangular punch problem

Young's modulus, $kg \cdot cm^{-1} \cdot s^{-2}$	$E = 1000$
Poisson's ratio	$\nu = 0.3$
Material density, $kg \cdot cm^{-3}$	$\rho = 0.01$
Punch angle	$\alpha = \tan^{-1} 2$

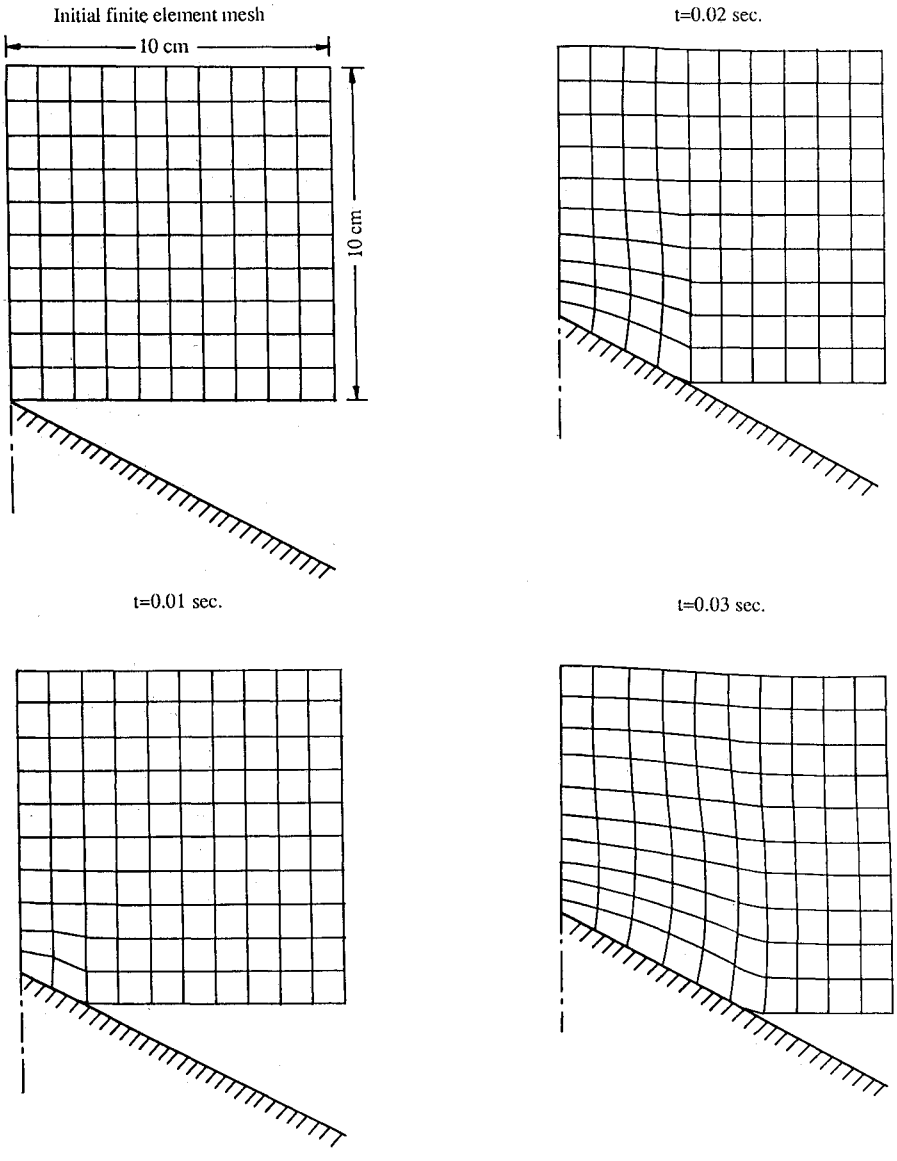

Fig. 9 Initial and deformed shapes for triangular punch problem.

contact pairs are consistent during contact. Once the release (0.205 s in Fig. 3 and 0.275 s in Fig. 4) occurs, the interface displacements of bar 2 are greater than those of bar 1, and this results in the separated displacement curves for Figs. 3 and 4.

Concentrated Mass Between Two Fixed Beams

The second model studied here is an H structure: a concentrated mass supported by two contact elements between two fixed beams as shown in Fig. 5. The dimensions and material properties are $A = 0.015$ in^2, $\rho_m = 7.34 \times 10^{-4}$ lb $\cdot$ s^2/in.^{4}, $EI = (1.03 \times 10^7) \cdot (1.125 \times 10^{-6})$ lb $\cdot$ in.^{2}, and damping $c = \beta[k^e] = 3.183 \times 10^{-5}[k^e]$. The concentrated mass weighs 1.82×10^{-3} lb $\cdot$ s^2/in., connected to the two beams using a soft spring and a contact spring. The stiffness of the soft spring is $k_0 = 1.758$ lb/in. The contact spring with the stiffness $k_1 = 175.8$ lb/in. in damping $c_1 = 7 \times 10^{-2}$ lb $\cdot$ s/in. is active when and only when the concentrated mass and the contact spring are in contact. The gap between the concentrated mass and the contact spring is taken as $\delta_0 = 0.02$ in.

The first five natural frequencies are evaluated using the NDAFEP,[1] SAP IV, the available analytical techniques, and our program NAS-JIGFEX. The results are summarized in Table 2.

A sinusoidal base excitation with an amplitude 0.1553 g and frequencies of 4 Hz and 3 Hz are applied to the base of the H structure. The displacements of the concentrated mass and two adjacent nodes on the contact spring are presented in Figs. 6 and 7. Similar results were also presented by Tzou and Schiff[1] using a pseudoforce approximation method.

It is already seen that the mass moves opposite to the base excitation and single contact for 4-Hz excitation and double contact for 3-Hz excitation within the half-cycle of excitation. Using the parametric quadratic programming method, it is guaranteed that the penetration does not occur to the contact processes because the penalty factor $E \to \infty$ is introduced. Hence, it can be observed that the "no penetration" condition is satisfied in Figs. 6 and 7.

Triangular Punch Problem

Finally, we consider the application of the algorithm to problems involving the frictional contact constraint. A rigid triangular punch is driven into a linear elastic half-plane at constant velocity $V = 100$ cm/s (see Fig. 8). The data for this problem is given in Table 3. Owing to the symmetry, only half of the elastic half-plane is modeled by 100 four-node plane-strain elements, and 11 contact elements are employed between the rigid punch and half-plane. No body forces and tractions are assumed to be applied.

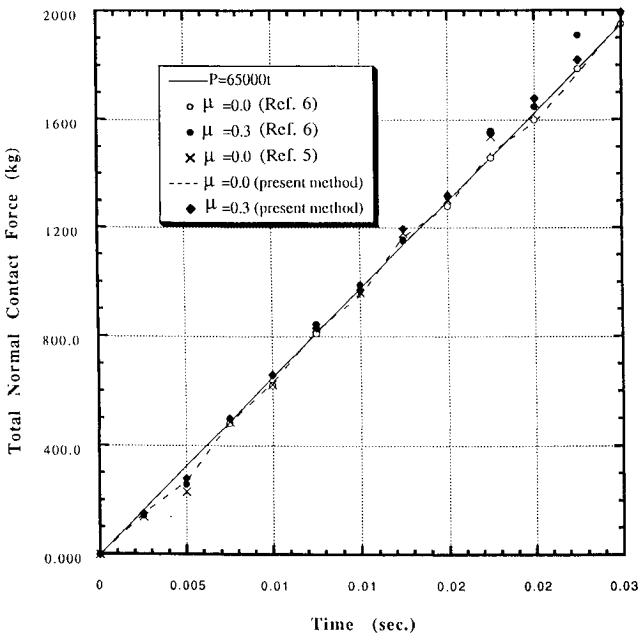

Fig. 10 Time variations of the total contact forces for triangular punch problem.

In the numerical experiment, both the frictionless case and the frictional case with $\mu = 0.3$ are examined. Figure 9 shows the initial finite element mesh and computed deformed shapes for the frictional case at the selected times. The total normal contact forces for two cases are displayed in Fig. 10, and the results are found to be in good agreement with those obtained by Hughes et al.[5] and Kanto and Yagawa.[6] Also, as seen in Fig. 10, the total normal contact force can be approximated to vary linearly with respect to time. Further, as expected, one observes that the frictional effect is to reduce the total normal contact force, although this reduction is small.

VII. Concluding Remarks

A parametric quadratic programming technique for the solution of frictional, damped elastodynamics contact systems has been presented. It evolves from earlier efforts found in Refs. 11–15 where the parametric variational principle and its numerical method are exploited: the parametric quadratic programming method solves the elasto-plastic structure,[15] the elasto-static contact,[12-14] and the elasto-plastic contact problem.[11] The solution of both the elasto-plastic structure and the contact problem can be described as a quadratic programming problem (48) with a parametric vector $\bar{\lambda}$.

$$\min[\Delta\pi(\Delta u) = \tfrac{1}{2}\Delta u^T K \Delta u - (\Phi\lambda + R)^T \Delta u \mid S\Delta u \le H\lambda + d] \quad (48)$$

Since the parametric vector λ satisfies

$$\lambda^T \bullet (H\lambda - S\Delta u + d) = 0, \qquad \lambda \ge 0 \quad (49)$$

The problem (48) can be treated as a linear complementary problem. The linear complementary problem can be solved by a well-known Lemke algorithm. Therefore, no preassigned tolerances are needed, and no trial solutions in the usual sense are performed.

The spatial and time discretization of the dynamic contact problem leads, at each time step, to the solution of the problem (48). Note that the "trial and error" method can be applied to the solved problem (48), but convergence to the correct solution does not occur in all cases. However, the linear complementary problem is solved with the Lemke method to a certain accuracy and numerical stability that guarantees the convergence of the nonlinear problem.

It should be emphasized that the substructure technique is adopted in the present work. For the dynamic contact problems, the numerical effort is considerable because of the nonlinear system equations at each time step. The substructure technique involved in the parametric quadratic programming method can reduce the computational scale of the nonlinear systems if nonlinearities are of a more local character.

Although all of the formulations were coded on a Silicon Graphics computer, we have favored the parametric quadratic programming method since it is much more inexpensive from the computational point of view. Moreover, it is easily implemented in an existing program, NAS-JIGFEX. In this paper, we discussed only one aspect of the dynamics contact analysis and parametric quadratic programming method. A number of additional problems on the mechanical as well as on the algorithmic side still deserve further work.

References

[1]Tzou, H. S., and Schiff, A. J., "Development and Evaluation of a Pseudo-force Approximation Applied to Nonlinear Dynamic Contact and Viscoelastic Damping," *Computers and Structures*, Vol. 26, No. 3, 1987, pp. 481–493.

[2]Carpenter, N. J., Taylor, R. L., and Katona, M. G., "Lagrange Constraints for Transient Finite Element Surface Contact," *International Journal for Numerical Methods in Engineering*, Vol. 32, No. 1, 1991, pp. 103–128.

[3]Ayari, M. L., and Saouma, V. E., "Static and Dynamic Contact/

Impact Problems Using Fictitious Forces," *International Journal for Numerical Methods in Engineering*, Vol. 32, No. 3, 1991, pp. 623-643.

[4]Kikuchi, N., and Oden, J. T., "Dynamic Friction Problems," *Contact Problems in Elasticity: A Study of Variational Inequalities and Finite Element Methods*, SIAM, Philadelphia, PA, 1988, pp. 409-430.

[5]Hughes, T. J., Taylor, R. L., Sackman, J. L., Curnier, A., and Kanoknukulchai, W., "A Finite Element Method for a Class of Contact Impact Problems," *Computer Methods in Applied Mechanics and Engineering*, Vol. 8, No. 8, 1976, pp. 249-276.

[6]Kanto, Y., and Yagawa, G., "A Dynamic Contact Buckling Analysis by the Penalty Finite Element Method," *International Journal for Numerical Methods in Engineering*, Vol. 29, No. 4, 1990, pp. 755-774.

[7]Kulak, R. F., "Adaptive Contact Elements for Three-dimensional Explicit Transient Analysis," *Computer Methods in Applied Mechanics and Engineering*, Vol. 72, No. 2, 1989, pp. 125-151.

[8]Sun, S. M., Natori, H. S., and Tzou, H. S., "Dynamic Analysis of Frames Taking into Account Contact and Viscoelastic Damping," *Procedings of the 34th JSASS/JSME Structures Conference*, Vol. B, Sapporo, Japan, 1992, pp. 94-97.

[9]Mahmoud, F. F., Hassan, M. M., and Salamon, N. J., "Dynamic Contact of Deformable Bodies," *Computers and Structures*, Vol. 36, No. 1, 1990, pp. 169-181.

[10]Talaslidis, D., and Panagiotopoulos, P. D., "A Linear Finite Element Approach to the Solution of the Variational Inequalities Arising in Contact Problems of Structural Dynamics," *International Journal for Numerical Methods in Engineering*, Vol. 18, No. 10, 1982, pp. 1505-1520.

[11]Zhong, W. X., and Sun, S. M., "A Finite Element Method for Elasto-plastic Structures and Contact Problems by Parametric Quadratic Programming," *International Journal for Numerical Methods in Engineering*, Vol. 26, No. 12, 1988, pp. 2723-2738.

[12]Zhong, W. X., and Sun, S. M., "A Parametric Quadratic Programming Approach to Elastic Contact Problems with Friction," *Computers and Structures*, Vol. 32, No. 1, 1989, pp. 37-43.

[13]Sun, S. M., "Quadratic Programming with Parametric Vectors in Three-dimensional Contact Problems," *Acta Mechanica Solida Sinica*, Vol. 2, No. 3, 1989, pp. 295-308.

[14]Sun, S. M., Qiu, C. H., and Zhong, W. X., "Mathematical Programming Method of Contact Problem in Rolling Bearing," *Chinese Journal of Mechanical Engineering*, Vol. 27, No. 1, 1991, pp. 42-48.

[15]Zhang, R. L., and Zhong, W. X., "The Numerical Solution for PMPEP by Parametric Quadratic Programming," *Computational Structural Mechanics and Applications*, Vol. 4, No. 1, 1987, pp. 1-12.

[16]Paz, M., "Reduction of Dynamic Matrices," *Structural Dynamics*, 2nd ed., Van Nostrand Reinhold, New York, 1985, pp. 247-274.

[17]Clough, R. W., and Penzien, J., "Variational Formulation of the Equation Motion," *Dynamics of Structures*, McGraw-Hill, New York, 1975, pp. 271-284.

[18]Björkman, G., "The Solution of Large Displacement Frictionless Contact Problems Using a Sequence of Linear Complementarity Problems," *International Journal for Numerical Methods in Engineering*, Vol. 31, No. 8, 1991, pp. 1553-1566.

[19]Klarbring, A., "A Mathematical Programming Approach to Three-dimensional Contact Problems with Friction," *Computer Methods in Applied Mechanics and Engineering*, Vol. 58, No. 2, 1986, pp. 175-200.

[20]Maier, G., and Munro, J., "Mathematical Programming Applications to Engineering Plastic Analysis," *Applied Mechanics Reviews*, Vol. 35, No. 12, 1982, pp. 1631-1643.